

# HIV treatment planning on a case-by-case basis

Marios M. Hadjiandreou, Raul Conejeros, and Ian Wilson

**Abstract**—This study presents a mathematical modeling approach to the planning of HIV therapies on an individual basis. The model replicates clinical data from typical-progressors to AIDS for all stages of the disease with good agreement. Clinical data from rapid-progressors and long-term non-progressors is also matched by estimation of immune system parameters only. The ability of the model to reproduce these phenomena validates the formulation, a fact which is exploited in the investigation of effective therapies. The therapy investigation suggests that, unlike continuous therapy, structured treatment interruptions (STIs) are able to control the increase in both the drug-sensitive and drug-resistant virus population and, hence, prevent the ultimate progression from HIV to AIDS. The optimization results further suggest that even patients characterised by the same progression type can respond very differently to the same treatment and that the latter should be designed on a case-by-case basis. Such a methodology is presented here.

**Keywords**—AIDS, chemotherapy, mathematical modeling, optimal control, progression.

## I. INTRODUCTION

**D**ESPITE the impressive amount of work in HIV research there are as yet no effective treatment strategies that prevent the ultimate progression from HIV to AIDS and death. Mathematical modeling can synthesize existing knowledge and provide a theoretical framework for the interpretation of existing paradigms. Furthermore, mathematical models can serve as a powerful tool in the quest for computing optimal treatment strategies due to their ability to estimate the patient's response to therapy [1].

It is important to validate any modelling attempt by using data from clinical trials or experimental studies. This has not been considered in most modeling work reported to date ([2]-[4]) yet is obviously essential in order to ensure that the model predictions replicate real phenomena. In addition, many studies did not consider the drug-resistant virus population ([2], [5]). The emergence of such a strain is known to be a key factor in the failure of current strategies and any proposed therapies that do not take this phenomenon into account are likely to be misleading. Furthermore, most studies [3] reported optimized strategies over very short treatment durations. Unless the goal of the study is to eradicate the virus or to achieve immunological control after cessation of treatment (this has as yet been proven to be very difficult to achieve due to the replication of virus in macrophages and long-lived cells ([6], [7]), optimal control studies should aim in designing a strategy which increases the long-term treatment benefit. Investigating short horizons might lead to

M.M. Hadjiandreou and D.I. Wilson are with the Department of Chemical Engineering and Biotechnology, University of Cambridge, UK (Tel: +44(0)1223 330 134; fax: +44(0)1223 334 796; e-mail: mmh38@cam.ac.uk).

R. Conejeros is with the Escuela de Ingenieria Bioquimica, Pontificia Universidad Catolica de Valparaiso, Chile (Tel: +56 32 2273652; e-mail: rconejer@ucv.cl).

results which are optimal over that short horizon but are not necessarily optimal in the long-term.

Many studies to date ([1], [2], [5]) considered the effect of treatment through an efficacy term. Different drugs, however, are associated with varied efficacies in the body as well as with different side-effects, hence, treatment planning ought to be drug-specific. Krakovska and Wahl [3] produced optimal strategies by considering the varied efficacies of different drugs, however, in their formulation all drugs carried a similar toxicity rating. This is rarely true and a side-effect index which takes into account the different toxicities associated with different drugs has to be considered. Lastly, no two individuals respond to infection and treatment in quite the same and a methodology which allows for patient-specific planning needs to be investigated.

We present here a mathematical model which considers all cell populations known to play a key role in HIV infection, including the drug-resistant virus population. The model is compared to literature-reported clinical data from different patients for the entire trajectory of the disease and used as a tool for the planning of treatment. The methodology proposed here allows for the formulation of long-term patient-specific drug-specific strategies. The paper is ordered as follows: Section I presents a mathematical modeling approach to the investigation of HIV treatment strategies, Section II presents the analysis of the optimal control results and a methodology for the formulation of therapy on an individual basis, Section III involves a discussion on the findings, and Section IV outlines the most important conclusions of this study.

## II. METHODS

### A. HIV dynamics

HIV infection can be characterised as a disease of the immune system, with progressive depletion of defensive cells, resulting in immunosuppression. Viruses cannot reproduce without the aid of living cells. HIV can infect a number of cells in the body, however, its main target are the CD4+ T-cells. HIV replicates inside infected cells and the newly-produced virus can now infect more cells. CD4+ T-cells are vital as they help facilitate the body's response to many common but potentially fatal infections. The HIV life cycle directly or indirectly causes a reduction in the number of these cells, rendering the body's immune system unable to defend itself against these infections. The key phenomena in the HIV infection cycle are illustrated in Fig. 1.

Once infected, the patient experiences a rapid decrease in the number of CD4+ T-cells, following a rapid increase in the virus population. The immune system (CTLs and macrophages) responds by killing infected cells and virus particles, causing a rapid increase in the number of T-cells. During

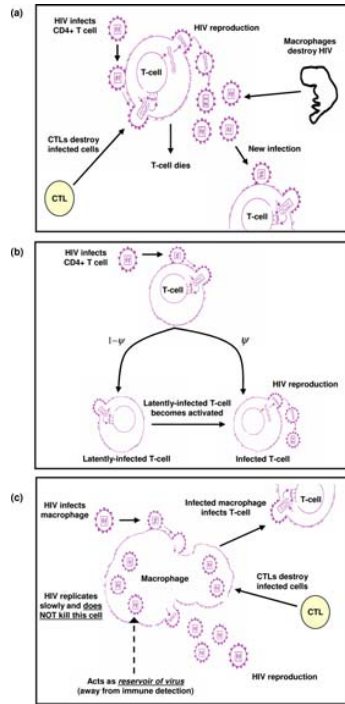


Fig. 1. Key phenomena during the course of HIV infection in (a) CD4+ T-cells, (b) latently-infected CD4+ T-cells, and (c) macrophages. Once infected a proportion  $1 - \psi$  of CD4+ T-cells passes into the latently-infected cell population. Reproduced from [9].

this time the virus population experiences a rapid depletion. A period of almost eight years follows (often referred to as the asymptomatic stage or latency) whereby CD4+ T-cells experience a constant but slow depletion. The virus infects more and more cells and thus slowly increases in number. After about eight years the immune system collapses and the virus population experiences an exponential growth. On the other hand, uninfected T-cells deplete at a high rate, crossing the  $200 \text{ mm}^{-3}$  line which marks the “progression to AIDS” period. Once patients are detected with AIDS, they survive for about one more year as suggested by [8]. Furthermore, once infected a proportion  $1 - \psi$  of CD4+ T-cells (Fig. 1(b)) passes into the latently-infected cell population. These latently-infected cells may be activated after a long time, and start reproducing virus.

During the course of HIV infection macrophages are also infected (Fig. 1(c)). The virus replicates slowly inside these cells and, unlike CD4+ T-cells, the macrophages are not killed but continue to accommodate more virus and protect it against immune responses and drugs. Also of importance is the fact that infected macrophages appear to be able to cause apoptosis of CD4+ T-cells [10]. Clinical studies [11] have suggested that during the late stages of the disease most virus comes from infected macrophages, hence the exponential rise.

### B. HIV model

The following components are considered:  $T$ , uninfected T-cells;  $T_1$ , T-cells infected by wild-type virus (drug-sensitive);

$T_2$ , T-cells infected by mutated virus (drug-resistant);  $T_{L1}$ , latently-infected T-cells infected by wild-type virus;  $T_{L2}$ , latently-infected T-cells infected by mutated virus;  $V_1$ , wild-type virus (drug-sensitive); and  $V_2$ , mutated virus (drug-resistant). The model also considers the uninfected and infected macrophage populations,  $M$ ,  $M_1$  and  $M_2$ , respectively, as well as the cytotoxic T-lymphocyte population,  $CTL$ . The governing set of differential equations is given by (1)-(11).

$$\frac{dT}{dt} = s_1 + \frac{p_1(V_1 + V_2)T}{V_1 + V_2 + S_1} - (1 - u_1)(k_1 V_1 + k_2 M_1)T - \varphi(k_1 V_2 + k_2 M_2)T + rT \left(1 - \frac{T + T_1 + T_2 + T_{L1} + T_{L2}}{T_{max}}\right) - \delta_1 T \quad (1)$$

$$\frac{dT_1}{dt} = (1 - u_1)\psi(k_1 V_1 + k_2 M_1)T + \alpha_1 T_{L1} - \delta_2 T_1 - k_3 T_1 CTL \quad (2)$$

$$\frac{dT_2}{dt} = \psi\varphi(k_1 V_2 + k_2 M_2)T + \alpha_1 T_{L2} - \delta_2 T_2 - k_3 T_2 CTL \quad (3)$$

$$\frac{dT_{L1}}{dt} = (1 - u_1)(1 - \psi)(k_1 V_1 + k_2 M_1)T - \alpha_1 T_{L1} - \delta_3 T_{L1} \quad (4)$$

$$\frac{dT_{L2}}{dt} = (1 - \psi)\varphi(k_1 V_2 + k_2 M_2)T - \alpha_1 T_{L2} - \delta_3 T_{L2} \quad (5)$$

$$\frac{dM}{dt} = s_2 + \frac{p_2(V_1 + V_2)M}{V_1 + V_2 + S_2} - (1 - f_1 u_1)k_4 V_1 M - \varphi k_4 V_2 M - \delta_4 M \quad (6)$$

$$\frac{dM_1}{dt} = (1 - f_1 u_1)k_4 V_1 M - \delta_5 M_1 - k_5 M_1 CTL \quad (7)$$

$$\frac{dM_2}{dt} = \varphi k_4 V_2 M - \delta_5 M_2 - k_5 M_2 CTL \quad (8)$$

$$\frac{dCTL}{dt} = s_3 + k_6(T_1 + T_2)CTL + k_7(M_1 + M_2)CTL - \delta_6 CTL \quad (9)$$

$$\frac{dV_1}{dt} = (1 - u_2)(1 - \mu)k_8 T_1 + (1 - f_2 u_2)(1 - \mu)k_9 M_1 + \mu\varphi k_8 T_2 + \mu\varphi k_9 M_2 - (k_{10}T + k_{11}M)V_1 - k_{12}V_1 M - \delta_7 V_1 \quad (10)$$

$$\frac{dV_2}{dt} = (1 - \mu)\varphi k_8 T_2 + (1 - \mu)\varphi k_9 M_2 + (1 - u_2)\mu k_8 T_1 + (1 - f_2 u_2)\mu k_9 M_1 - (k_{10}T + k_{11}M)V_2 - k_{12}V_2 M - \delta_7 V_2 \quad (11)$$

(1) characterises the changes in the uninfected T-cell population,  $T$ . The first two terms on the RHS of (1) represent the sources of new T-cells. They incorporate cells from the thymus, bone marrow, and general production. It is assumed that there exists a constant thymic source,  $s_1$ , as well as a proliferation term due to an immune response. T-cells have finite lifespans; the average of which is  $1/\delta_1$ , where  $\delta_1$  is the death rate of the uninfected T-cells. The last two terms on the RHS of (1) represent the infection of T-cells by both virus and infected macrophages (drug-sensitive and drug-resistant strain). Constant rates of infectivity  $k_1$  and  $k_2$  are assumed. Consideration of macrophages is regarded essential since this population plays a vital role in HIV progression. The logistic term in (1) does not allow the T-cell population to exceed a maximum concentration,  $T_{max}$  following antiretroviral treatment ([12],[13]).

(2)-(5) describe changes in the infected and latently-infected T-cell populations,  $T_1$ ,  $T_2$ ,  $T_{L1}$ ,  $T_{L2}$ . The first term on the RHS of the equations represents the increase in number of infected cells. Once infected, a proportion of T-cells,  $\psi$ , passes into the infected T-cell population, whereas a proportion  $1 - \psi$  passes into the latently-infected T-cell population. These latently-infected cells might become activated after a long time and start reproducing virus. This activation is represented through

the  $\alpha_1 T_{L1}$  and  $\alpha_1 T_{L2}$  terms in (2)-(5). Infected cells are lost by such processes such as natural death and immune responses. The rate at which CTLs kill infected T-cells is given by  $k_3$  in (2)-(3).

The population of macrophages increases in terms of the constant source of new cells,  $s_2$ , and its increase due to the immune response (6). The latter term depends on the number of virus particles and the increase rate,  $p_2$ . According to [10], when T-cells signal macrophages that the virus is non-self (*i.e.*, an 'invader'), the latter divide and become more aggressive. Thus, it was considered essential to include this behaviour in the model. Macrophages are lost through infection by virus at a rate of  $k_4$ , and through natural death at a rate of  $\delta_4$ . In (7) and (8) the gain terms carry over from the loss terms in (6). Infected macrophages (both strains) are lost to natural death and to immune responses. The rate at which CTLs kill infected macrophages is given by  $k_5$ .

The rate of change of CTLs is given by (9). These cells are generated at a constant rate,  $s_3$ , and proliferate with a rate described by rate constants,  $k_6$  and  $k_7$ , proportional to the current amount of the same infected T-cells and infected macrophages, respectively. CTLs die at a rate  $\delta_6$ .

(10) and (11) describe the rate of change in the drug-sensitive ( $V_1$ ) and drug-resistant ( $V_2$ ) virus population, respectively. These populations increase due to production of virus from drug-sensitive and drug-resistant infected T-cells and macrophages, respectively. For example, the amount of  $V_2$  produced from  $T_2$  and  $M_2$  is given by  $(1 - \mu)k_8 T_2$  and  $(1 - \mu)k_9 M_2$ , respectively, where  $k_8$  and  $k_9$  are the rates of production per unit time in T-cells and macrophages. The amount of  $V_2$  produced from  $T_1$  and  $M_1$  is given by  $\mu k_8 T_1$  and  $\mu k_9 M_1$ , respectively, where  $\mu$  represents the percentage of virus mutation ( $V_1$  to  $V_2$ , and vice versa). Virus is lost through the terms  $k_{10} V_i T$  and  $k_{11} V_i M$ , effectively accounting for the virus lost when infecting T-cells and macrophages without producing new virus, *e.g.*, as a result of the infected cell's natural death or through the action of CTLs. Virus is also lost through natural death ( $\delta_7 V_i$ ) as well as through an immune response ( $k_{12} V_i M$ ).

Viral mutations are accounted in the model via the parameter  $\mu$ , which represents the probability of a mutation per replication cycle ( $V_1$  to  $V_2$ , and vice-versa). This approach has also been used in other studies ([14], [15]) and takes indirectly into account the mutations occurring in both the transcription and production stage of the replication cycle. The reduced fitness of  $V_2$  in terms of infecting and replicating capacity is considered in the model equations above through parameter  $\varphi$ .

Parameters  $u_1$  and  $u_2$  ( $u_1, u_2 \in [0, 1]$ , with 0 and 1 indicating no treatment and full treatment, respectively) represent the efficacy of reverse transcriptase inhibitors (RTI) and protease inhibitors (PI), respectively. RTIs inhibit the infection of T-cells and macrophages by virus whereas the PIs inhibit the production of infectious virus from already infected cells. It is important to note that these drugs have no effect on the resistant virus population. Treatment on macrophages is not as effective as that on T-cells hence, the term  $f_i u_i$  [2]. Estimation of drug efficacies in the body requires use of a

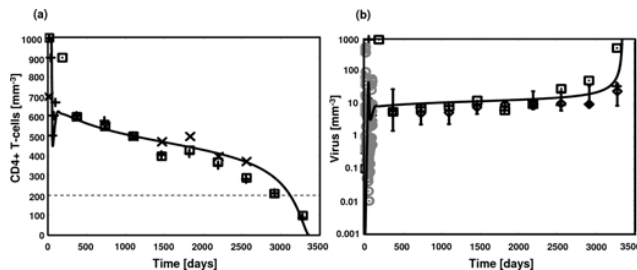


Fig. 2. Concentration-time profiles for (a) CD4+ T-cell and (b) virus for an untreated typical-progressor to AIDS. Model predictions from Hadjiandreou *et al.* [23]. Comparison with clinical data from the studies by [18] (+), [24] (o), [25] (◇), [19] (x), and [20] (□). Dotted line marks progression to AIDS.

TABLE I

PARAMETER VALUES USED IN THE MODEL. UNLESS OTHERWISE STATED, BEST FIT VALUES ESTIMATED (EST.) FROM CLINICAL DATA OF T-CELLS ([18], [19], [20]) WHEN NO TREATMENT IS USED.

Parameter	Value	Source	Literature	Units
$s_1$	10	[13]	5 – 36	$\text{mm}^{-3}\text{d}^{-1}$
$s_2$	0.15	[13]	0.03 – 0.15	$\text{mm}^{-3}\text{d}^{-1}$
$s_3$	5	Est.	–	$\text{mm}^{-3}\text{d}^{-1}$
$p_1$	0.16	Est.	0.01 – 5	$\text{d}^{-1}$
$p_2$	0.15	Est.	–	$\text{d}^{-1}$
$S_1$	55.6	Est.	1 – 188	$\text{mm}^{-3}$
$S_2$	188	Est.	–	$\text{mm}^{-3}$
$k_1$	$3.87 \times 10^{-3}$	Est.	$10^{-8} - 10^{-2}$	$\text{mm}^3\text{d}^{-1}$
$k_2$	$1 \times 10^{-6}$	[13]	$10^{-6}$	$\text{mm}^3\text{d}^{-1}$
$k_3$	$4.5 \times 10^{-4}$	Est.	$10^{-4} - 1$	$\text{mm}^3\text{d}^{-1}$
$k_4$	$5.22 \times 10^{-4}$	Est.	$4.7 \times 10^{-9} - 10^{-3}$	$\text{mm}^3\text{d}^{-1}$
$k_5$	$3 \times 10^{-6}$	Est.	–	$\text{mm}^3\text{d}^{-1}$
$k_6$	$3.3 \times 10^{-4}$	Est.	$10^{-6} - 10^{-3}$	$\text{mm}^3\text{d}^{-1}$
$k_7$	$6 \times 10^{-9}$	Est.	–	$\text{mm}^3\text{d}^{-1}$
$k_8$	$5.37 \times 10^{-1}$	Est.	$2.4 \times 10^{-1} - 5 \times 10^2$	$\text{d}^{-1}$
$k_9$	$2.85 \times 10^{-1}$	Est.	$5 \times 10^{-3} - 3 \times 10^2$	$\text{d}^{-1}$
$k_{10}$	$7.79 \times 10^{-6}$	Est.	$10^{-8} - 10^{-2}$	$\text{mm}^3\text{d}^{-1}$
$k_{11}$	$1 \times 10^{-6}$	Est.	$4.7 \times 10^{-9} - 10^{-3}$	$\text{mm}^3\text{d}^{-1}$
$k_{12}$	$4 \times 10^{-5}$	Est.	–	$\text{mm}^3\text{d}^{-1}$
$\delta_1$	0.02	[13]	0.01 – 0.02	$\text{d}^{-1}$
$\delta_2$	0.28	Est.	0.24 – 0.7	$\text{d}^{-1}$
$\delta_3$	0.05	Est.	0.02 – 0.069	$\text{d}^{-1}$
$\delta_4$	$5 \times 10^{-3}$	[13]	0.005	$\text{d}^{-1}$
$\delta_5$	$5 \times 10^{-3}$	[13]	0.005	$\text{d}^{-1}$
$\delta_6$	0.015	[21]	0.015 – 0.05	$\text{d}^{-1}$
$\delta_7$	2.39	[13]	2.39 – 13	$\text{d}^{-1}$
$\alpha_1$	$3 \times 10^{-4}$	Est.	–	$\text{d}^{-1}$
$\psi$	0.97	Est.	0.93 – 0.98	–
$\varphi$	0.9	[22]	0.1 – 0.9	–
$r$	0.03	[13]	0.03	$\text{d}^{-1}$
$T_{max}$	1500	[13]	1500 – 2000	$\text{mm}^{-3}$
$\mu$	0.001	[14]	$3 \times 10^{-5} - 1 \times 10^{-3}$	–
$f_i$	0.34	[2]	0.34	–

pharmacokinetic model which is described in Appendix A.

In specifying model parameters and initial conditions for the model, estimated values were generated from clinical data of T-cell dynamics of typical-progressors when no therapy is used. This was done using a least-squares method code written in *Mathematica 5.1<sup>TM</sup>* [16]. Some parameter values were taken directly from the literature. Estimates of parameter values are given in Table I. Furthermore,  $T(0) = 1000 \text{ mm}^{-3}$ ,  $M(0) = 30 \text{ mm}^{-3}$ ,  $V_1(0) = 0.001 \text{ mm}^{-3}$  [13], and  $CTL(0) = 333 \text{ mm}^{-3}$  [17]. It should be noted that the initial concentrations for the infected populations and  $V_2$  were set to 0.

Fig. 2 presents data from five clinical studies representing the typical progression of the disease, with the results of the model given for direct comparison. The predictions for the T-cells and virus populations show good agreement with clinical data for HIV-infected patients during the same time period. It is important to note that although clinical data for the T-cells alone were used in the parameter estimation, the model is able to replicate clinical data for the virus population as well, including the exponential rise of the virus towards the end-stages of the disease. This further validates the modeling work in this study.

### C. Rapid-progressors and long-term non-progressors

In this section, we investigate the ability of the model to replicate clinical data from other progressors to AIDS, namely rapid-progressors (RPs) and long-term non-progressors (LTNPs). RPs are those patients whose T-cell levels decrease below the threshold of AIDS after approximately 3-5 years [5]. These constitute a small proportion (10% [26]) of infected individuals. The majority of patients progress to AIDS within 8-10 years after initial infection and are known as typical-progressors (see above). LTNPs are a small proportion (10-17% [26]) of the infected population who evade the typical progression to AIDS without the help of therapy for as long as 15-20 years ([5], [27]). The differences in the rate of progression between individuals has been suggested to be based on factors such as immune system's status, age, and genetic profile ([5], [28]). Here, the parameters associated with the immune system alone are estimated using a least-squares code written in *Mathematica 5.1<sup>TM</sup>*; namely, the action of the CTLs ( $k_3, k_5$ ) and macrophages ( $k_{12}$ ) on the infected cells and virus, respectively, as well as the increase of uninfected cells (T-cells, macrophages, and CTLs) as part of the immune response ( $p_1, p_2, S_1, S_2, k_6$ , and  $k_7$ ). The estimated parameter values are listed in Table II with plots depicting cell population concentration-time profiles for both RPs and LTNPs shown in Fig. 3. Clinical data for T-cell dynamics from RPs and LTNPs have been plotted alongside model results for comparison.

It is important to note the effect of the immune system parameters on the degree of progression to AIDS. For the RP, a reduction in these parameters (*e.g.*, 12% decrease of proliferation rate of CTLs,  $k_6$  and  $k_7$ ) results in a weaker immune response (Fig. 3(c)), hence, an increased virus load

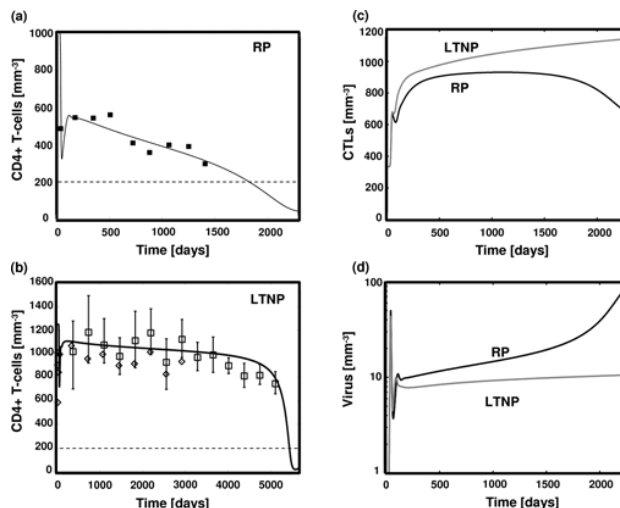


Fig. 3. Concentration-time profiles for T-cells (a-b), CTLs (c), and total virus (d) for an untreated RP and LTNP. Comparison with clinical data from the clinical studies by [29] (■), [18] (◇), and [30] (□). The data from [30] involved 7 patients, hence the mean and standard error bars. Dotted line marks progression to AIDS.

(Fig. 3(d)) and a more rapid decline in the T-cell count (Fig. 3(a)). Model results for T-cell dynamics show good agreement with clinical data from one patient. For the LTNP case, an increase in the immune system parameters (*e.g.*, 10% increase in  $k_6$  and  $k_7$ ) results in a stronger immune response (Fig. 3(c)), hence, a reduced virus load (Fig. 3(d)) and a considerably slower depletion of T-cells (Fig. 3(b)). It is worth noting the difference in the life expectancies of the three types of progressors (RP: 6 years, typical: 9.5 years, LTNP: 15.5 years). Model results for the T-cell dynamics have been compared with clinical data from patients displaying LTNP characteristics with good agreement. This match of clinical data further validates the modeling work in this study, which is able to replicate the dynamics of different types of progressors. This has been achieved by estimating only the parameters associated with the immune system response. The performance of the immune system has been suggested ([5], [24]) to be one of the main factors determining the degree of progression to AIDS, and the ability of the model to reproduce some features of this phenomenon further validates its application.

### D. Drug Related side-effects

An optimal strategy clearly involves the successful control of the disease. Another parameter which has to be considered in the formulation of treatment strategies, however, is the intensity of the drug-related side-effects. Neglecting this might prove fatal to the patient. The relationship between antiretroviral drugs and their side-effects is well documented [31]. Table III summarises the observed side-effects as a result of three widely used antiretroviral drugs at standard dosage (one PI, RDV, and two RTIs, 3TC and ZDV). More specifically, the table summarises the observed frequency of the side-effect within a population as well as its relative magnitude. The latter is clearly subjective, *e.g.*, "chills" should be less

TABLE II

PARAMETER VALUES USED IN THE MODEL FOR A RP AND A LTNP. THE VALUES OF THE REMAINING PARAMETERS ARE SIMILAR TO THE ONES FOR THE TYPICAL-PROGRESSOR'S CASE (TABLE I).

Parameter	RP	Typical-progressor	LTNP	Units
$p_1$	0.13	0.16	0.2	$d^{-1}$
$p_2$	0.1365	0.15	0.1638	$d^{-1}$
$S_1$	50.0	55.6	55.6	$mm^{-3}$
$S_2$	169.2	188	188	$mm^{-3}$
$k_3$	$3.96 \times 10^{-4}$	$4.5 \times 10^{-4}$	$9.9 \times 10^{-4}$	$mm^{-3}$
$k_5$	$2.64 \times 10^{-6}$	$3 \times 10^{-6}$	$6.6 \times 10^{-6}$	$mm^{-3}$
$k_6$	$2.9 \times 10^{-4}$	$3.3 \times 10^{-4}$	$3.63 \times 10^{-4}$	$mm^{-3}$
$k_7$	$5.28 \times 10^{-9}$	$6 \times 10^{-9}$	$6.6 \times 10^{-9}$	$mm^{-3}$
$k_{12}$	$3.52 \times 10^{-5}$	$4 \times 10^{-5}$	$4.4 \times 10^{-5}$	$mm^{-3}$
$r$	0.03	0.03	0.072	$d^{-1}$

undesirable than an “increase in blood sugar” or ”diaorrhea”. A drug-specific side-effect index formulation in an attempt to investigate the impact of side-effects in the optimal design of treatment strategies is presented in Appendix B.

III. RESULTS AND DISCUSSION

Here, patient and drug-specific optimal treatment profiles for HIV-infected patients employing a widely used drug regime (RDV, 3TC, ZDV) and drug concentrations as controls are generated using *gPROMS 3.0.3* [33]. In this work, an optimal treatment is one that prolongs progression to AIDS so as to evade opportunistic infections, maintains a high CD4+ T-cell count, as well as reduces the impact of drug-associated side-effects.

A. Structured treatment interruptions

Hadjiandreou *et al.* [9] involved the investigation of treatment strategies using drug efficacies as controls. Both continuous therapy and STIs were considered and the results suggested that, unlike continuous therapy, STIs are very effective in controlling disease progression. It was suggested that the key to the successful implementation of STI therapy, which is not as yet included in antiretroviral guidelines, is the optimal management of the magnitude and frequency of treatment interruptions in an attempt to facilitate the interplay between the drug-sensitive and drug-resistant virus strains. In this way, neither the sensitive nor the resistant strain increase and disease progression can be controlled as a result.

That work is extended here by the formulation of a dynamic optimization problem of STI therapy for the case of a typical-progressor (see Fig. 2 and Table I) using the drug-specific model presented earlier. The optimal control problem takes the form of OCP1:

$$\begin{aligned}
 & \text{OCP1} \\
 & \max_{c_1, c_2, c_3} J(t_f, \mathbf{C}) \\
 \text{s. t.} \quad & J(t_f, \mathbf{C}) = \int_{t_0}^{t_f} [A_1 T - A_2 S_e] dt \quad (12) \\
 & \dot{\mathbf{x}} = f(t, \mathbf{x}, \mathbf{C}), \\
 & T \geq T_{AIDS}, \\
 & t \in [t_0, t_f]
 \end{aligned}$$

where  $\dot{\mathbf{x}} = f(t, \mathbf{x}, \mathbf{C})$  represents the governing set of equations ((1)-(11), (13)-(18)),  $t \in [t_0, t_f]$  sets the finite horizon of the optimization, and  $T_{AIDS}$  defines the condition for the undesirable transition from HIV to full-blown AIDS. The benefit of treatment is based on the maximisation of T-cells and the minimisation of the severity of side-effects associated with the drug regime over the treatment horizon. A fixed life expectancy of 10,000 days (~28 years) after initial infection is assumed. Bearing in mind that current treatment strategies extend life expectancy to a maximum of around 19 years depending on the type of patient and drug regime used ([34]-[36]), it is believed that an estimated life expectancy of ~28 years after initial infection is a realistic target to consider.

Like other problems of discontinuous nature, optimization of the pharmacokinetics during multiple doses adds further

TABLE III  
 FREQUENCIES AND ESTIMATED RELATIVE MAGNITUDE OF THREE WIDELY USED DRUGS. SIDE-EFFECT REPORTED IN > 15% (x) OF INDIVIDUALS, 5 - 15 % (□), < 5% (●), AND SIDE-EFFECT NOT REPORTED IN INDIVIDUALS (+). SIDE-EFFECT IS CONSIDERED “STRONGLY UNDESIRABLE” (\*\*\*), UNDESIRABLE (\*\*), AND “WEAKLY UNDESIRABLE” (\*).

SIDE-EFFECT	DRUG		
	RDV	3TC	ZDV
<b>Following laboratory tests</b>			
Anemia **	●	●	×
Leukopenia **	●	●	×
Neutropenia **	●	□	×
Thrombocytopenia **	●	●	●
↑ Alkaline Phosphatase **	●	+	+
↑ Amylase (pancreas) **	●	●	+
↑ Bilirubin (liver) **	●	●	●
↑ Cholesterol ***	×	+	+
↑ Creatinine (kidney) **	□	+	+
↑ Glucose (blood sugar) ***	+	+	+
↑ Liver functions **	□	●	×
↑ Triglycerides **	×	+	+
<b>As symptoms</b>			
Abdominal pain **	□	□	×
Altered taste *	×	+	□
Anorexia **	□	□	×
Arthralgia **	●	□	×
Chills *	●	□	×
Constipation *	●	+	●
Depression *	●	□	●
Diaorrhea ***	×	×	×
Dizziness **	□	□	□
Fatigue **	×	×	□
Fevers **	●	□	×
Headache **	□	×	×
Insomnia *	●	□	□
Malaise **	□	×	×
Menstrual irregularities *	×	+	+
Myalgia (muscle pain) **	□	□	×
Nausea ***	×	×	×
Nephrolithiasis **	+	+	+
Neurological symptoms ***	□	●	●
Neuropathy **	●	□	●
Pancreatitis ***	●	□	+
Paresthesia **	×	+	●
Rash ***	●	□	×
Seizures *	+	+	+
Vomiting ***	×	□	□

Reproduced from [31] and [32]

complexity to the problem. The latter is already quite complicated due to the highly non-linear nature of the system of equations involved. In order to reduce the complexity associated with modeling pharmacokinetics in the optimization, the concentration of drug *i* during dosage interval  $\tau$  is modelled as following an average concentration during that time interval. Moreover, the treatment levels are fixed during the optimization in an attempt to reduce the complexity further. Administration of fixed drug dosages over treatment intervals also helps compliance from clinicians and patients.

Treatment initiation occurs at  $T < 350 \text{ mm}^{-3}$  (Antiretroviral Guidelines [37]) with fixed values for average  $C_1, C_2,$  and  $C_3$  at  $[0.0472, 0.0205, 0.00659]^T$  and  $[0.0, 0.0, 0.0]^T$  during ON and OFF treatment, respectively. Given initiation at  $T < 350 \text{ mm}^{-3}$  these values (equivalent to  $\mathbf{u} = [0.1, 0.3]^T$ ) were found (using optimization) to be the minimum concentrations that are able to achieve the target life expectancy of 10,000 days. The ON and OFF periods are allowed to vary between  $10 \leq ON, OFF \leq 150$  days, thereby excluding

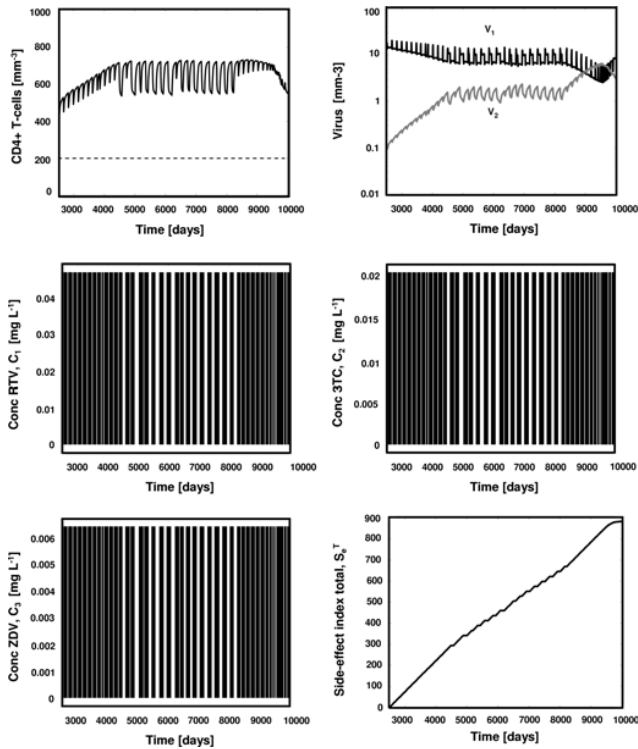


Fig. 4. Optimal control profiles of  $C_1$ ,  $C_2$ , and  $C_3$  for STIs for a treatment-naive typical-progressor. Objective function:  $J(t_f, \mathbf{u}) = \int_{t_0}^{t_f} [A_1 T - A_2 S_e] dt$ . Initiation of therapy is at  $T < 350 \text{ mm}^{-3}$  ( $\sim 2,500$  days after initial infection). Shaded region indicates treatment spell. Dotted line marks progression to AIDS.

extended periods of OFF treatment that could be fatal to the patient ([38], [39]). Since the magnitudes of the T-cell population and the side-effect index are on different scales, weighting values  $A_1 = 1 \text{ mm}^3$  and  $A_2 = 1,000$  are used. The optimization solution is sensitive to an increase in  $A_2$ , with low administration of both drugs as  $A_2$  increases (results not shown). Lower T-cell population numbers are achieved as a result. The number of control intervals used is 100 and the piecewise-constant profiles obtained are presented in Fig. 4. The total CPU time required for this optimization was 280.2 s.

The results depicted in Fig. 4 suggest that STIs are very effective in controlling disease progression in HIV-infected patients. Neither the drug-sensitive nor the drug-resistant virus strain grows in an uncontrolled manner and as a result the T-cell count is maintained above the threshold of AIDS for longer. During the early stages of optimised STIs, the schedule requires maximum ON (150 days) and minimum OFF (10 days) periods. This slows down the increase of the drug-sensitive strain, which is the main problem for a patient that has not developed any resistance. The optimized schedule is successful in reducing the total ON treatment to 74% of total therapy and the total side-effect index in this STI scenario is 880. In way of comparison, the  $S_e^T$  value obtained under current continuous treatments (600 mg RDV, 150 mg 3TC, 300 mg ZDV, twice daily) for the same treatment horizon

was 3,640. This suggests that, on top of extending the life-expectancy of patients considerably, the optimized schedules presented here are able to reduce the impact of drug-associated side-effects markedly. In doing this, the patients also enjoy an increased number of drug-free periods. All these imply that the optimal strategies proposed here offer a considerable advantage to the patient.

### B. Patient-specific treatment

So far, the optimal strategies proposed have been formulated for patients displaying the general characteristics of typical-progressors (the majority of patients in this category progress to AIDS after  $\sim 10$  years). No two individuals respond to infection and treatment in quite the same way, however, and this section investigates to what extent these strategies are able to extend the life-expectancy of other patients. Furthermore, this section presents a methodology for the formulation of patient-specific treatment planning.

The patient involved in this section is taken from the study by [40]. This patient falls in the category of typical-progressors (progression to AIDS after 5-15 years; [5], [26]), however, it is clear that progression to AIDS occurs considerably earlier for this individual (after  $\sim 5$  years; see Fig. 5) when compared to the majority of typical-progressors (progression after  $\sim 10$  years; see Fig. 2). The concentration-time profile for T-cells for this patient as predicted by the therapy model is presented in Fig. 5. In replicating the observed clinical data, only the immune system parameters (reduced proliferation of immune cells,  $p_1, p_2, S_1, S_2, k_6, k_7$ ; action of CTLs and macrophages,  $k_3, k_5, k_{12}$ ) have been altered (see Table IV); it is believed that this patient exhibited a weaker immune status [6], hence the faster progression to AIDS.

Treatment is initially administered according to the general STI schedule reported in Fig. 4. The results are not encouraging; the projected survival-time after initial infection for this patient is 2,800 days (Fig. 6(a)), hence, the proposed schedule is not effective in extending the time before progression to AIDS occurs noticeably.

These results confirm that a general treatment framework is not effective and treatment has to be assessed on an individual basis. Optimal treatment planning for a specific patient involves: (a) monitoring the T-cell count of the individual down to  $T = 350 \text{ mm}^{-3}$ , (b) prediction of HIV dynamics specific to that individual by fitting the model to data, and (c) formulation

TABLE IV  
PARAMETER VALUES FOR AN UNTREATED PATIENT FROM THE STUDY BY [40]. THE REMAINDER OF THE PARAMETER VALUES ARE SIMILAR TO THE ONES FOR THE TYPICAL-PROGRESSOR'S CASE (TABLE I)

Parameter	Value	Units
$p_1$	0.19	$\text{d}^{-1}$
$p_2$	0.15	$\text{d}^{-1}$
$S_1$	55.6	$\text{mm}^{-3}$
$S_2$	188	$\text{mm}^{-3}$
$k_3$	$4.16 \times 10^{-4}$	$\text{mm}^{-3}$
$k_5$	$2.78 \times 10^{-6}$	$\text{mm}^{-3}$
$k_6$	$3.01 \times 10^{-4}$	$\text{mm}^{-3}$
$k_7$	$5.5 \times 10^{-9}$	$\text{mm}^{-3}$
$k_{12}$	$3.7 \times 10^{-5}$	$\text{mm}^{-3}$

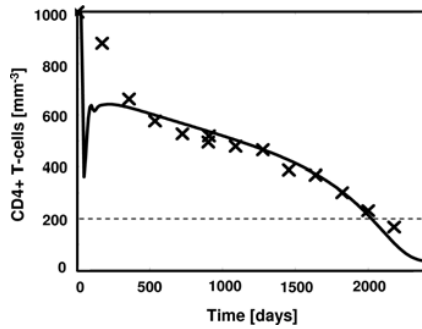


Fig. 5. Uninfected T-cell concentration-time profile over the course of HIV infection for an untreated patient from the study by [40] (x). Results have been obtained by fitting the model to the data down to  $T = 350 \text{ mm}^{-3}$ . Results show good agreement with the remaining data ( $T < 350 \text{ mm}^{-3}$ ). Dotted line marks progression to AIDS.

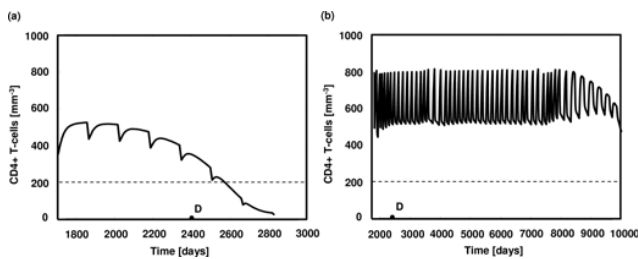


Fig. 6. Treatment studies on the patient [40] depicted in Fig. 5. Initiation of therapy is at  $T < 350 \text{ mm}^{-3}$  ( $\sim 1,700$  days after initial infection). Application of (a) STI schedule reproduced from Fig. 4 for a typical-progressor and (b) patient-specific optimal treatment. Dotted line marks progression to AIDS. Point D indicates projected survival-time when no treatment is administered.

of the patient-specific treatment strategy initiated at  $T < 350 \text{ mm}^{-3}$ . In the case of the patient in this section, the model predictions in Fig. 5 have been obtained by fitting the model to the data down to  $T = 350 \text{ mm}^{-3}$ , and the predictions show good agreement with the remaining data in Fig. 5 (for  $T < 350 \text{ mm}^{-3}$ ). The patient-specific optimal treatment was then formulated and when administered was able to prolong the progression to AIDS to more than 10,000 days (Fig. 6(b)), thereby emphasising the importance of formulating treatment schedules on an individual basis.

The results presented in this study are based on the predictions of mathematical models. Such models offer a simplified description of reality, as do virtually all modeling attempts. The present work has only dealt with the infection of CD4+T-cells and macrophages. Other cells (e.g., dendritic cells) may become infected and may exhibit different kinetics. Also, direct cell-to-cell transmission of virus has not been considered and death of cells due to effects other than direct viral killing and natural death has been ignored. Furthermore, time delays should also be considered, hence, treating interactions between cells, virus, and drugs as non-instantaneous [8]. As far as the immune response is concerned, the effect of the suppressor cells has been assumed to be minimal compared to that of the CTLs. Furthermore, we have no control over the fitness of the drug-resistant strain [22]. In fact, mutations at every fitness level are likely to occur and the optimal treatment would be

different in that case. Lastly, the drug-resistant virus has been modelled as one that has developed resistance to all drugs in an attempt to formulate optimal treatment strategies for this group of patients. This constitutes a large percentage of HIV-infected patients [41], nevertheless, inclusion of variables describing different drug-resistant strains is likely to result in a model which describes reality more closely. Another assumption in the model is lack of terms describing ageing factors. The age/ageing of individuals has been suggested [28] to be an important factor determining disease progression and response to treatment. In this work, the schedules run over long periods of time and the parameters are likely to change as the individual involved ages. As a result, the treatment might not necessarily be completely effective for the entire treatment horizon and a model accounting for this is likely to result in further improved predictions. We acknowledge these concerns and investigation of the results presented in this work through clinical or experimental studies is highly desirable.

#### IV. CONCLUSION

In this study an optimal control approach was considered in an attempt to formulate HIV treatment strategies. The optimization results suggest that a general treatment protocol cannot be proposed and treatment planning has to be produced on a case-by-case basis. Drug-specific treatment involves consideration of a side-effect index by using a well-documented side-effect chart whereas patient-specific treatment involves firstly the estimation of the patient-specific model parameters using clinical data, and subsequently the formulation of the treatment. The results presented in this work identified considerable scope for the improvement of current treatments, extending survival-time considerably and reducing the index associated with the side-effects of drugs markedly. The results suggest that STI therapy offers a promising alternative to current guidelines and should encourage further experimental and clinical work for validation purposes.

#### APPENDIX A

##### PHARMACOKINETIC MODEL

Drug efficacies are given as a function of the concentration and effectiveness of the drug. For the drug regime involved (one PI: RDV, two RTIs: 3TC, ZDV), the RTI and PI efficacies are given by [42]:

$$u_1(t) = \frac{(C_2(t)/IC_{50}^2) + (C_3(t)/IC_{50}^3)}{1 + (C_2(t)/IC_{50}^2) + (C_3(t)/IC_{50}^3)} \quad (13)$$

$$u_2(t) = \frac{C_1(t)}{C_1(t) + \omega IC_{50}^1} \quad (14)$$

where  $u_1(t)$  and  $u_2(t)$  range from 0 to 1 and indicate RTI and PI efficacy, respectively, and  $C_i(t)$  and  $IC_{50}^i$  indicate plasma and median inhibitory drug concentrations, respectively.

(14) presents a pharmacokinetic model describing drug concentration in the peripheral blood as a function of drug dosage. For simplicity, concentrations are modelled using a one-compartment open model with first-order absorption and elimination [42] and fixed pharmacokinetic parameters. Let  $C_i(t)$  be the plasma concentration of drug  $i$  at time  $t$ . The

model between dosages, (*i.e.*,  $t_l < t < t_{l+1}$ ) can be written as follows [42]:

$$C_i(t) = C_i(t_l) e^{-k_e^i(t-t_l)} + \frac{F_i D_i}{V_c^i} \frac{k_a^i}{k_a^i + k_e^i} [e^{-k_e^i(t-t_l)} - e^{-k_a^i(t-t_l)}] \quad i \in N, l \in n \quad (15)$$

where  $i$  is the index that denotes drugs;  $t_l$  is the time at which dose  $D_i$  is administered;  $F_i$  is the absolute bioavailability of drug  $i$  (the fraction of dose available);  $k_a^i$  is the absorption rate of drug  $i$ ;  $k_e^i = \frac{Cl_i}{V_c^i}$  is the elimination rate constant of drug  $i$ ;  $Cl_i$  is the clearance of drug  $i$ ;  $V_c^i$  is the volume of distribution of drug  $i$ ;  $C_i(t_0) = 0$ ; and  $Cl_i, V_c^i, k_a^i > 0$ .

The model in (15) is solved in *Mathematica 5.1<sup>TM</sup>* for the drug regime consisting of RDV, 3TC, and ZDV and the results are plotted alongside respective clinical data with considerable agreement (Fig. 7(i)). The pharmacokinetic parameters used in the model are consistent with the manufacturers' recommendations ([44], [45]) and are given in Table V. For illustrative purposes, the time-course of concentrations of these drugs (all administered twice daily at standard dosage according to antiretroviral guidelines) over the first 3 days of dosing is plotted in Fig. 7(ii).

APPENDIX B

SIDE-EFFECT INDEX FORMULATION

The side-effect of a drug regime at a given time is given as a function of the concentrations of the drugs involved, the relative magnitude of the side-effect, and its observed frequency within a population. This has been presented previously in a review study [32] and is given in (16):

$$S_e(t) = \sum_{i=1}^N \bar{e}_i \frac{C_i(t)}{C_i} \quad (16)$$

$$\bar{e}_i = \frac{e_i}{\max_{i \in N}(e_i)} \quad i \in N \quad (17)$$

$$e_i = \sum_{j \in J_i} (q_j \cdot h_{i,j}) \quad i \in N \quad (18)$$

In this system of equations, the side-effect index,  $S_e(t)$ , represents the magnitude of the side-effect of a drug regime at time  $t$ .  $J_i$  is the set of side-effects related to drug  $i$ ,  $C_i(t)$  is the concentration of drug  $i$  at time  $t$ ,  $\bar{C}_i$  is the mean concentration of drug  $i$  at steady-state at standard dosage (*i.e.*, according to

TABLE V

PARAMETER VALUES USED IN THE PHARMACOKINETIC MODEL. VALUES TAKEN FROM THE PRODUCT INFORMATION OF THE MANUFACTURERS ([44], [45]). PARAMETER  $\tau$  REPRESENTS THE DOSING INTERVAL OF THE PROPOSED DRUG REGIME.

Parameter	RDV, $C_1$	3TC, $C_2$	ZDV, $C_3$
$D$ [mg]	600	150	300
$k_a$ [ $d^{-1}$ ]	2.4	12	12
$Cl$ [ $L d^{-1}$ ]	$1.48 \times 10^4$	$5.6 \times 10^2$	$2.69 \times 10^3$
$V_c$ [L]	28.7	91	112
$F$	1.0	0.86	0.64
$\tau$ [d]	1/2	1/2	1/2
$IC_{50}$ [ $mg L^{-1}$ ]	0.11	0.34	0.13

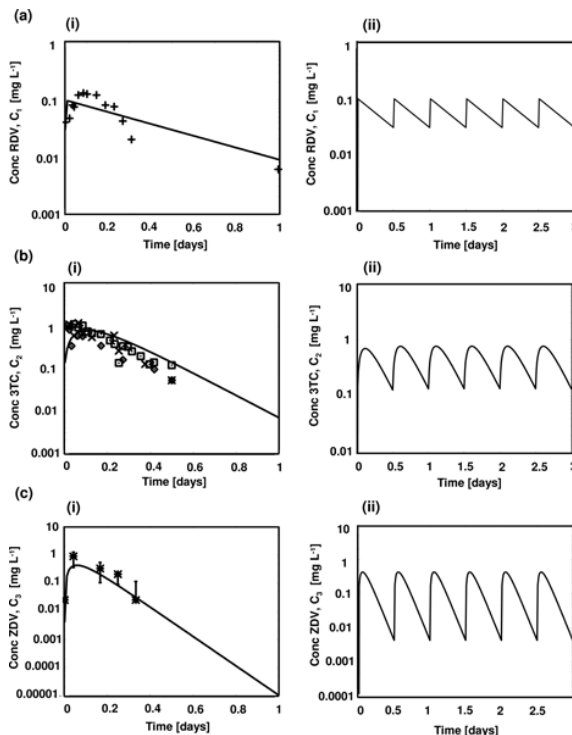


Fig. 7. (i) Model predictions for the concentration of three drugs (a-c) during treatment at standard dosage and steady-state conditions. Comparison with clinical data from: [46] (\*), [47] (+), and [48] (x, diamond, square). (ii) Time-course of plasma concentrations of (a) RDV, (b) 3TC, and (c) ZDV at standard dosage over the first 3 days of dosing.

antiretroviral guidelines),  $e_i(\bar{e}_i)$  is the magnitude (normalised magnitude) of the side-effect caused by drug  $i$  at standard dosage,  $h_{i,j}$  is the frequency of individuals that present side-effect  $j$  when subject to drug  $i$  at standard dosage, and  $q_j$  is the relative magnitude of side-effect  $j$ , *i.e.*, “undesirability”. This model is based on the additivity of the observed frequencies and magnitudes of side-effects, and considers that the magnitude of the side-effect index is proportional to the amount of drug administered. When solving the system of equations (16)-(17) above, the relative magnitudes of side-effects are modelled as 0.1, 0.2, and 0.7 for “weakly undesirable”, “undesirable”, and “strongly undesirable”, respectively. Although fuzzy logic techniques [43] may be used to describe the transition from one state to another (*e.g.*, “undesirable” to “strongly undesirable”), this basic “metric” approach is considered here in order to reduce complexity. Furthermore, the observed frequencies of side-effects are modelled using values of 0, 0.05, 0.15, and 0.6 to represent the case where “side-effect has not been reported in individuals”, “side-effect reported in less than 5% of individuals”, “side-effect reported from 5% up to 15% of individuals”, and “side-effect reported in more than 15% of individuals”, respectively.

ACKNOWLEDGMENT

This work was supported by grants from Alexander S. Onasis Benefit Public Foundation, the Cambridge Commonwealth



Trust, and the Centre of Latin American Studies, University of Cambridge. The authors would also like to thank the Chilean Governmental Research Fund (FONDECYT 1080118) for funding the collaboration visits to the UK.

## REFERENCES

- [1] S. Khalili and A. Armaou, "An extracellular stochastic model of early HIV infection and the formulation of optimal treatment policy", *Chem. Eng. Sci.*, vol. 63, pp. 4361-4372, 2008.
- [2] B. M. Adams, H. T. Banks, and H. Kwon, "Dynamic multidrug therapies for HIV: optimal and STI control approaches", *Math. Biosci. Eng.*, vol. 1, pp. 223-241, 2004.
- [3] O. Krakovska and L. M. Wahl, "Drug-sparing regimens for HIV combination therapy: benefits predicted for drug coasting", *Bull. Math. Biol.*, vol. 69, pp. 2627-2647, 2007.
- [4] L. Rong, M. A. Gilchrist, Z. Feng, "Modelling within-host HIV-1 dynamics and the evolution of drug resistance: trade-offs between viral enzyme function and drug susceptibility", *J. Theor. Biol.*, vol. 247, pp. 804-818, 2007.
- [5] S. H. Bajaria, G. Webb, M. Cloyd, "Dynamics of nave and memory CD4+ T lymphocytes in HIV-1 disease progression", *JAIDS*, vol. 30, pp. 41-58, 2002.
- [6] S. H. Bajaria, G. Webb, and D. E. Kirschner, "Predicting differential responses to structured treatment interruptions during HAART", *Bull. Math. Biol.*, vol. 66, pp. 1093-1118, 2004.
- [7] T. W. Chun, R. Davey, and D. Engel, "Re-emergence of HIV after stopping therapy", *Nature*, vol. 401, pp. 874-875, 1999.
- [8] M. A. Nowak and A. J. McMichael, "How HIV defeats the immune system", *Scientific American*, pp. 58-65, 1995.
- [9] M. M. Hadjiandreou, R. Conejeros, and D. I. Wilson, "Long-term HIV dynamics subject to continuous therapy and structured treatment interruptions", *Chem. Eng. Sci.*, vol. 64, pp. 1600-1617, 2009.
- [10] M. A. Nowak, R. M. May, "Virus dynamics: Mathematical principles of immunology and virology", New York: Oxford University Press, 2000.
- [11] T. Igarashi, C. R. Brown, Y. Endo, "Macrophages are the principal reservoir and sustain high virus loads in rhesus macaques following the depletion following the depletion of CD4+ T-cells by a highly pathogenic SHIV: implications for HIV-1 infections of man", *PNAS*, vol. 98, pp. 658-663, 2001.
- [12] K. S. Dorman, A. H. Kaplan, K. Lange, "Mutation takes no vacation: can structured treatment interruptions increase the risk of drug-resistant HIV-1?", *JAIDS*, vol. 25, pp. 398-402, 2000.
- [13] D. E. Kirschner and A. S. Perelson, "A model for the immune system response to HIV: AZT treatment studies", In: O. Arino, D. Axelrod, M. Kimmel, editors, *Mathematical population dynamics: analysis of heterogeneity and theory of epidemics*, Winnipeg: Wuerz Publishing, pp. 295, 1995.
- [14] D. E. Kirschner and G. F. Webb, "A mathematical model of combined drug therapy of HIV infection", *J. Theor. Med.*, vol. 1, pp. 25-34, 1997.
- [15] J. Velasco-Hernandez, J. A. Garcia, and D. E. Kirschner, "Remarks on modeling host-viral dynamics and treatment", In: C. Chavez, S. Blower, P. Van Den Dreische, editors, *Mathematical Approaches for Emerging and Reemerging Infectious Diseases: An Introduction to Models, Methods and Theory*, vols. 1 and 2, New York: Springer-Verlag, 2001.
- [16] Wolfram Research, Inc., *Mathematica, Version 5.1*, Champaign, IL, U.S, 2004.
- [17] F. M. Campello de Souza, "Modeling the dynamics of HIV-1 and CD4 and CD8 lymphocytes", *IEEE Eng. Med. Biol.*, vol. 18, pp. 21-24, 1999.
- [18] A. S. Fauci, G. Pantaleo, S. Stanley, "Immunopathogenic mechanisms of HIV infection", *Annals of Internal Medicine*, vol. 124, pp. 654-663, 1996.
- [19] J. B. Margolick, A. D. Donnenberg, and A. Munoz, "T Lymphocytes homeostasis after seroconversion", *JAIDS*, vol. 7, pp. 415-416, 1994.
- [20] E. Pennisi, J. Cohen, "Eradicating HIV from a patient: not just a dream?", *Science*, vol. 272, pp. 1884, 1996.
- [21] E. Vergu, A. Mallet, and J. Golmard, "A modeling approach to the impact of HIV mutations on the immune system", *Comput. Biol. Med.*, vol. 35, pp. 1-24, 2005.
- [22] R. F. Stengel, "Mutation and control of the human immunodeficiency virus", *Math. Biosci.*, vol. 213, pp. 93-102, 2008.
- [23] M. M. Hadjiandreou, R. Conejeros, and V. S. Vassiliadis, "Towards a long-term model construction for the dynamic simulation of HIV infection", *Math. Biosci. Eng.*, vol. 4, pp. 489-504, 2007.
- [24] R. A. Filter, X. Xia, and C. M. Gray, "Dynamic HIV/AIDS parameter estimation with application to a vaccine readiness study in Southern Africa", *IEEE Trans. Biomed. Eng.*, vol. 52, pp. 784-791, 2005.
- [25] C. A. Sabin, H. Devereux, A. N. Phillips, "Course of viral load throughout HIV-1 infection", *JAIDS*, vol. 23, pp. 172-177, 2000.
- [26] S. LeBlanc, "The long and the short of AIDS Progression", *The Bay Area Reporter*, 1996.
- [27] M. Comar, C. Simonelli, S. Zanussi, "Dynamics of HIV-1 mRNA expression in patients with long-term nonprogressive HIV-1 infection", *J. Clin. Invest.*, vol. 100, pp. 893-900, 1997.
- [28] T. E. Yamashita, J. P. Phair, A. Munoz, "Immunologic and virologic response to highly active antiretroviral therapy in the Multicenter AIDS Cohort Study", *AIDS*, vol. 15, pp. 735-746, 2001.
- [29] R. B. Markham, W. Wang, A. E. Weisstein, "Patterns of HIV-1 evolution in individuals with differing rates of CD4 T cell decline", *PNAS*, vol. 95, pp. 12568-12573, 1998.
- [30] T. C. Greenough, D. B. Brettler, F. Kirchhoff, "Long-term non-progressive infection with human immunodeficiency virus type in a hemophilia cohort", *J. Infect. Dis.*, vol. 180, pp. 1790-1802, 1999.
- [31] The Body Health Resources Corporation, Drug Side Effects Chart, [Online] Available: <http://www.thebody.com/pinf/sideeffectchart.html> (accessed in 2007).
- [32] M. Joly and J. M. Pinto, "Role of mathematical modeling on the optimal control of HIV-1 pathogenesis", *AICHEJ*, vol. 52, pp. 856-885, 2006.
- [33] gPROMS Advanced User Guide, Release 2.3. 2004. Process System Enterprise Ltd, United Kingdom.
- [34] R. S. Braithwaite, A. C. Justice, C. C. Chang, "Estimating the proportion of patients infected with HIV who will die of comorbid diseases", *Am. J. Med.*, vol. 118, pp. 890-898, 2005.
- [35] C. T. Fang, H. M. Hsu, S. J. Twu, "Decreased HIV transmission after policy of providing free access to highly active antiretroviral therapy in Taiwan", *J. Infect. Dis.*, vol. 190, pp. 879-885, 2004.
- [36] A. D. Paltiel, M. C. Weinstein, A. D. Kimmel, "The qualitative nature of the primary immune response to HIV infection is a prognosticator of disease progression independent of the initial level of plasma viremia", *PNAS*, vol. 94, pp. 254-258, 1997.
- [37] "Antiretroviral Guidelines 2006". Department of Health and Human Services, pp. 1-113. [Online] Available: <http://www.aidsinfo.nih.gov/ContentFiles/AdultandAdolescentsGL.pdf>. Accessed (March 2007).
- [38] J. Lawrence, D. L. Mayers, K. H. Hullsiek, "Structured treatment interruption in patients with multidrug-resistant human immunodeficiency virus", *N. Engl. J. Med.*, vol. 349, pp. 837-846, 2003.
- [39] L. Ruiz, E. Ribera, A. Bonjoch, "Role of structured treatment interruption before a 5-drug salvage antiretroviral regimen: the retrogene study", *J. Infect. Dis.*, vol. 188, pp. 977-985, 2003.
- [40] T. Hraba, J. Dolezal, "A mathematical model and CD4+ lymphocyte dynamics in HIV infection", *Em. Infect. Dis.*, pp. 299-305, 1996.
- [41] UK Group on Transmitted HIV Drug Resistance, "Time trends in primary resistance to HIV drugs in the United Kingdom: multicentre observational study", *BMJ*, vol. 331, pp. 1368-1371, 2005.
- [42] Y. Huang, S. L. Rosenkranz, H. Wu, "Modeling HIV dynamics and antiviral response with consideration of time-varying drug exposures, adherence, and phenotypic sensitivity", *Math. Biosci.*, vol. 184, pp. 165-186, 2003.
- [43] V. Novk, I. Perfilieva, and J. Mockor, *Mathematical principles of fuzzy logic*, USA: Kluwer Academic Publishers, 1999.
- [44] GlaxoSmithKline, Product Information. 2005. [Online] Available: <http://www.gsk.com/products/prescriptionmedicines.shtml>.
- [45] Abbott Laboratories, Product Information. 2006. [Online] Available: <http://www.norvir.com/hiv/hiv0044.htm>.
- [46] F. T. Aweeka, M. Kang, J-Y Yu, "Pharmacokinetic evaluation of the effects of ribavirin on zidovudine triphosphate formation: ACTG 5092s Study Team", *HIV Medicine*, vol. 8, pp. 288-294, 2007.
- [47] B. S. Kappelhoff, A. D. R. Huitema, K. M. L. Crommentuyn, "Development and validation of a population pharmacokinetic model for ritonavir used as a booster or as an antiviral agent in HIV-1-infected patients", *Br. J. Clin. Pharmacol.*, vol. 59, pp. 174-182, 2004.
- [48] M. Legrand, E. Comets, G. Aymard, "An in vivo pharmacokinetic/pharmacodynamic model for antiretroviral combination", *HIV Clin. Trials*, vol. 4, pp. 170/183, 2003.

**Marios M. Hadjiandreou** Dr. Hadjiandreou's research interests and expertise include the application of mathematical modeling and optimization techniques in biomedicine. Marios holds a PhD from the University of Cambridge and an MEng in Chemical Engineering from Imperial College London, UK.

**Raul Conejeros** Professor Raul Conejeros is a Professor of Biochemical Engineering at the Pontificia Universidad Catolica de Valparaiso in Chile. He holds a Diploma in Biochemical Engineering from PUCV and a PhD in Chemical Engineering from the University of Cambridge.

**D. Ian Wilson** Dr. Wilson is a Reader in Chemical Engineering at the University of Cambridge. He holds an MEng from the University of Cambridge and a PhD from the University of British Columbia, both in Chemical Engineering. Dr. Wilson is a Fellow of the Institution of Chemical Engineers, UK.